

Article

Multiagent-Based Distributed Coordination of Inverter-Based Resources for Optimal Operation of Microgrids Considering Communication Failures[†]

Woon-Gyu Lee¹, Thai-Thanh Nguyen² and Hak-Man Kim^{1,3,*}

¹ Department of Electrical Engineering, Incheon National University, 119 Academy-ro, Yeonsu-gu, Incheon 22012, Korea; dltnlqpf@inu.ac.kr

² Department of Electrical and Computer Engineering, Clarkson University, Potsdam, NY 13699, USA; tnguyen@clarkson.edu

³ Research Institute for Northeast Asian Super Grid, Incheon National University, 119 Academy-ro, Yeonsu-gu, Incheon 22012, Korea

* Correspondence: hmkim@inu.ac.kr; Tel.: +82-32-835-8769; Fax: +82-32-835-0773

[†] The present work is an extension of the paper “Distributed Optimal Control Strategy of Multiagent-Based Microgrid System Considering Communication Failure” presented to APAP 2021 Conference, Jeju, Korea, 11–14 October 2021.

Abstract: This paper proposes the distributed coordination of inverter-based resources, to optimize the operational cost of a microgrid system. The microgrid is considered a multiagent system, which includes a distributed generator agent and energy storage system agent. A communication network is utilized to exchange information among agents. The issue of communication failures is addressed in the proposed strategy, to ensure the stable operation of the control system. A two-level hierarchical cooperative optimization system is proposed in this paper for distributed economic dispatch. The primary controller is responsible for the frequency and voltage regulations, and the secondary controller is implemented in a diffusion-based distributed control scheme, for optimal microgrid management. The proposed control strategy consistently maintains the optimal operation and frequency, even in the event of communication failures. A five-node multiagent system including a dispatchable agent is considered. Comparative studies with the conventional consensus strategy are represented, to prove the effectiveness of the proposed diffusion strategy. To demonstrate the practical feasibility of the proposed strategy, a controller hardware-in-the-loop testbed was developed for testing the proposed cyber-physical microgrid system, in which the controllers were implemented in multiple computers and the microgrid system was implemented in Opal-RT. The real-time experiment results showed the better cost optimization performance of the proposed diffusion strategy compared with the conventional consensus strategy.

Keywords: microgrid; distributed control; diffusion algorithm; multi-agent cooperative control; economic dispatch; frequency control



Citation: Lee, W.-G.; Nguyen, T.-T.; Kim, H.-M. Multiagent-Based Distributed Coordination of Inverter-Based Resources for Optimal Operation of Microgrids Considering Communication Failures. *Energies* **2022**, *15*, 3736. <https://doi.org/10.3390/en15103736>

Academic Editor: Abdul-Ghani Olabi

Received: 29 March 2022

Accepted: 17 May 2022

Published: 19 May 2022

Publisher’s Note: MDPI stays neutral with regard to jurisdictional claims in published maps and institutional affiliations.



Copyright: © 2022 by the authors. Licensee MDPI, Basel, Switzerland. This article is an open access article distributed under the terms and conditions of the Creative Commons Attribution (CC BY) license (<https://creativecommons.org/licenses/by/4.0/>).

1. Introduction

A microgrid (MG) is a networked power system composed of various inverter-based distributed energy resources (DER), an energy storage system (ESS), and the load [1]. With the increase in DER, MG systems have become increasingly complex, in terms of overall operation and control [2]. As interactions between the power generation source, load, and power network of the MG system occur frequently, stably controlling various DERs, as well as economical operation plans, are key issues [3–5]. MG systems generally contain both dispatchable and non-dispatchable agents. Thus, economic dispatch (ED) is used to perform optimal management for controlling the power output of all DERs. In a distributed control strategy used to resolve the economic dispatch problem (EDP), all devices are involved in solving the generation cost optimization, reducing the computational burden

on the controller, and improving the reliability of the control system. Since each device exchanges information through communication with neighboring devices, a plug-and-play function is possible, which has easy scalability. An intelligent MG system can be used to efficiently solve the optimization problem through a distributed communication network [6]. A multiagent system (MAS) strategy is usually adopted for the integrated operation of various distributed power sources. MAS performs information exchange through peer-to-peer (P2P) communication, by regarding each distributed generation source as an agent [7–9].

Recently, various distributed optimization strategies have been proposed to resolve the EDP in a MG system. A distributed consensus and innovation framework strategy for the EDP of power systems is proposed in [10]. In [11–14], a distributed incremental cost consensus (ICC) algorithm was proposed, based on the Lagrange multiplier method, which is mainly used for centralized systems. The incremental cost value of the quadratic cost function was computed according to the output power of each DER. The consensus algorithm converges variables to the same point through iterative computations based on a communication network with neighboring agents. A performance verification of the ICC algorithm was performed with various communication topologies in [15–18]. The convergence rate of the consensus algorithm was determined by the communication network and the number of agents, and this affects the control performance of the MG system. The diffusion strategy was adopted to improve the convergence speed of the distributed optimization algorithm [19–21]. The diffusion algorithm is an effective strategy for solving the deterministic optimization, by considering a set of interacting agent networks [22]. These strategies typically require a load prediction technique to satisfy power balancing constraints and optimize operations in load uncertainty. The load prediction step requires an additional control layer, with increasing complexity and additional cost for the MG system. In [23], a two-step diffusion strategy was proposed, to determine the total load of the MG system, and solve the EDP optimization. A distributed control strategy, including an economic dispatch algorithm and frequency deviation optimization, was proposed to avoid the load prediction step in [24]. These studies only focused on the EDP optimization and frequency regulation, while the distributed communication failure of the MG system was not considered.

The optimal operation of the distributed system is affected by to the stability of the secondary communication system between agents. When a communication system fails, the information exchanged with other agents becomes corrupted and the optimal operation to address EDP fails. Thus, it is important to handle failures in the communication link by ensuring that a reliable bidirectional flow of data is transmitted to the secondary controller of each agent. Recently, various papers on cyber-attacks and line failures in communication systems have been proposed for distributed control systems [25–29]. In [25], the effect of communication failure on a distributed control system was analyzed and a MG modeling architecture was proposed to improve the system stability during communication degradation. In [26], a distributed robust ED method was proposed, to solve energy management. This paper implemented a fully distributed system that was robust against various collusive and non-collusive attacks. The impact of various types of cyber-attack on communication auxiliary controllers with potential vulnerabilities was analyzed, and a framework for ensuring system stability when a communication link was subjected to such attacks was proposed in [27]. An event-based distributed consensus frequency control strategy for inverter-interfaced distributed generators under a harsh communication system was proposed in [28]. The paper integrated event-based data and communication topology update mechanisms to improve the adaptability of control strategies in unreliable system conditions. In [29], a resilient distributed control strategy was proposed that allows each participant in a distributed control system to detect and isolate compromised links and controllers. These control strategies were designed to satisfy the operational goal, by isolating the line in which the communication error is detected. When an error occurs in the communication module of a single agent, the communication lines with

the neighboring agent are isolated. However, an agent isolated due to a communication failure can no longer exchange information with other agents, which adversely affects the optimal operating solution of the MG system operation. Thus, the isolation strategy of the agent whose communication failure is detected has limitations, in terms of optimizing the generation cost.

To overcome these limitations, this paper proposes a multiagent-based distributed optimization strategy, including compensation for frequency deviation according to the incremental cost. Since the total demand power and the output of all agents are correlated with the system frequency, it is possible to estimate the output power required for an isolated agent [30]. Thus, this paper performs the re-optimization process by deriving the incremental cost using the frequency deviation, as much as the output of the isolated agent. Compared to the conventional strategy, the proposed strategy consistently maintains the economic operation and demand load balance of the MG system, even in the event of a communication failure. The simulation results for verifying the controller performance when considering the proposed communication failure were compared with the conventional consensus-based distributed optimization strategy. Furthermore, real-time experimental results were obtained on a hardware-in-the-loop (HIL) test platform, where the MAS communication network system was implemented. The main contributions of this study are listed as follows:

- A multiagent-based distributed control strategy is proposed to optimally manage the MG system, even with communication failure;
- The proposed strategy does not require a load forecasting model to optimize the microgrid operation, due to the involvement of a secondary frequency regulator in the optimization process;
- A controller hardware-in-the-loop simulation platform was developed to validate the operating performance of the proposed multiagent control system.

The rest of this paper is organized as follows: Section 2 represents the hierarchical control structure of the proposed strategy, including the incremental cost diffusion algorithm. The proposed distributed multiagent system based on the diffusion algorithm is described in Section 3. The simulation results and comparison results are provided in Section 4. The experiment of the distributed communication system is presented in Section 5. Finally, the main conclusion of this study is summarized in Section 6.

2. MAS Structure for the EDP

The MG system of MAS consists of dispatchable and non-dispatchable agents. In the MAS framework, each DER device can be assigned an intelligent agent that connects with neighboring devices to achieve operational optimization. Each agent uses the distributed communication to share its own information, and the economic operation process aims to minimize the total generation cost, while maintaining the system frequency adjustment in the MG system in the event of a communication failure. A multiagent-based distributed control system consists of a hierarchical control structure.

2.1. MG System Control Hierarchy

In this study, Figure 1 presents the two-level hierarchical control layers of the MG system, which are divided into a primary control layer and secondary control layer. The device layer includes dispatchable agents consisting of three diesel generators (DGs) and two energy storage systems (ESS). The primary controller (PC) is mainly responsible for the demand power balance and power quality maintenance in islanded operation. The secondary controller (SC) is responsible for economic operation based on the incremental cost. The control sequence of the hierarchical control layers is shown in Figure 2, in which two layers are executed with different sampling times, to prevent interference with the optimization of the lower control layer. The primary control layer has a short control interval (T_s), as it needs an immediate response speed to balance the demand load, while the

secondary control layer operates at a relatively long control interval (T_p), as it determines the power reference ($P_i^*[k + 1]$) based on incremental cost.

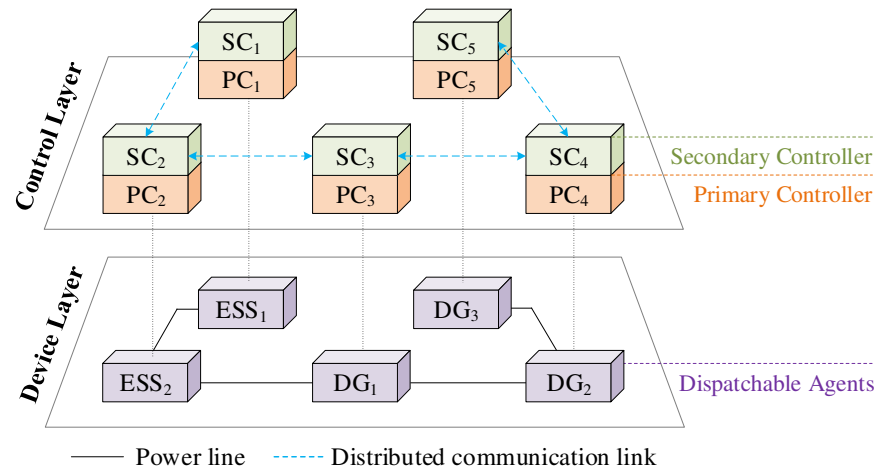


Figure 1. Scheme of the multiagent system.

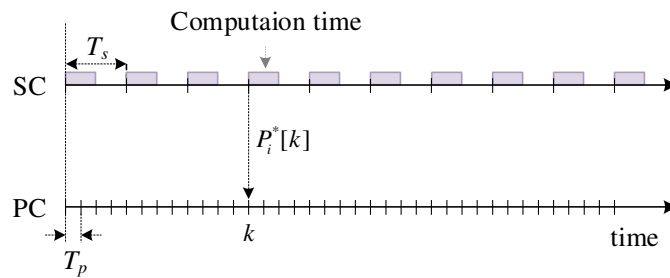


Figure 2. Control strategy with two layers, with a different sampling layer.

2.2. Agent Description

Each type of device connected to the MG system node has its cost function for operational optimization. According to the system components, the cost functions of the following two types of agents are defined [31]:

- Distributed generator agents

The distributed generator agents manage the output according to the generation power reference from the upper layer. The generation cost is typically expressed according to the active power output, as given by (1). The Lagrange multiplier method is utilized to resolve the cost objective function. Considering the derivative of each variable in the cost function, the quadratic cost function given in Equation (1) can be rewritten as (2). The generation output of the agent for operational optimization is limited, as in (3).

$$C(P_d^{DG}) = \alpha_d \cdot (P_d^{DG})^2 + \beta_d \cdot P_d^{DG} + \gamma_d \tag{1}$$

$$\frac{\partial C(P_d^{DG})}{\partial P_d^{DG}} = 2\alpha_d \cdot P_d^{DG} + \beta_d \tag{2}$$

$$P_{d,min}^{DG} \leq P_d^{DG} \leq P_{d,max}^{DG} \tag{3}$$

where $C_d(P_d^{DG})$ is the quadratic cost function of each diesel generator; P_d^{DG} is the output power of d -th DG; α_d , β_d , and γ_d are the quadratic cost coefficients; $\partial C_d(P_d^{DG}) / \partial P_d^{DG}$ is the incremental cost function; and $P_{d,min}^{DG}$ and $P_{d,max}^{DG}$ are the lower and upper limits of the agent output power, respectively.

- Energy storage system agents

The ESS agent has a bidirectional function of absorbing or compensating power, to balance the power demand of the system. In an MG system, the battery typically charges when the incremental cost is low, and discharges when the cost is high. The state of health (SOH) is related to the wearing cost, which is determined by the depth of discharge (DOD) in each cycle and the number of operation cycles. The cost of charging or discharging the battery is affected by the remaining SOC of each interval. Therefore, the DOD-based ESS cost function considering SOH can be expressed as a quadratic function, as in (4). The incremental cost of ESS is as shown in Equation (5), and battery charging and discharging are limited as in (6).

$$C(P_e^{ESS}) = x_e \cdot \left(P_e^{ESS} + 3P_{e,\max}^{ESS} \cdot (DOD) \right)^2 + y_e \cdot \left(P_e^{ESS} + 3P_{e,\max}^{ESS} \cdot (DOD) \right) + z_e \quad (4)$$

$$\frac{\partial C(P_e^{ESS})}{\partial P_e^{ESS}} = 2x_e \left(P_e^{ESS} + 3P_{e,\max}^{ESS} \cdot (DOD) \right) + y_e \quad (5)$$

$$-P_{e,\max}^{ESS} \leq P_e^{ESS} \leq P_{e,\max}^{ESS} \quad (6)$$

where $C_e(P_e^{ESS})$ is the quadratic cost function of the energy storage agent; P_e^{ESS} is the charging or discharging power; $P_{e,\max}^{ESS}$ is the upper bound; x_e , y_e , and z_e are the coefficients of quadratic generation cost; and $\partial C_e(P_e^{ESS})/\partial P_e^{ESS}$ is the incremental cost of the ESS, defined as the derivative of the quadratic cost function.

3. Proposed Distributed Control Strategy

In this paper, the DER of the MG system has five agents, composed of three DGs and two ESSs. Each agent device is implemented as an inverter-based power source, to improve control performance. The overall control diagram of the distributed generation agent based on the hierarchical control scheme is shown in Figure 3. The control system is implemented as a separate module of the primary controller and the secondary controller. A droop controller is applied at the primary control layer, for power sharing between DGs. In the secondary controller, a diffusion-based distributed controller is implemented for economic optimization and incremental cost-based frequency regulation, considering a communication failure. Figure 4 presents the information-sharing flow chart of the proposed secondary control layer in this study. In the first step, each agent receives information from its neighbors to update the number of agents and weight matrix. In the second step, the demand net power (P_D) is computed by the diffusion algorithm, and the incremental cost (λ_i) of each agent is computed based on the current output. Diffusion-based distributed cost optimization is performed to maintain the rated frequency in the third step. Through the rated frequency compensation process, demand net power and output are matched, without additional load forecasting. The communication connection status with the neighbors is checked in the fourth step. When a communication line failure is detected, a re-optimization process, including an incremental cost adjustment term considering frequency deviation, is performed for continuous cost optimization. In the fifth step, the power reference (P^*) is determined based on the converged incremental cost and sent to the primary controller. Finally, the output power of the agent is measured and sent to the adjacent agents.

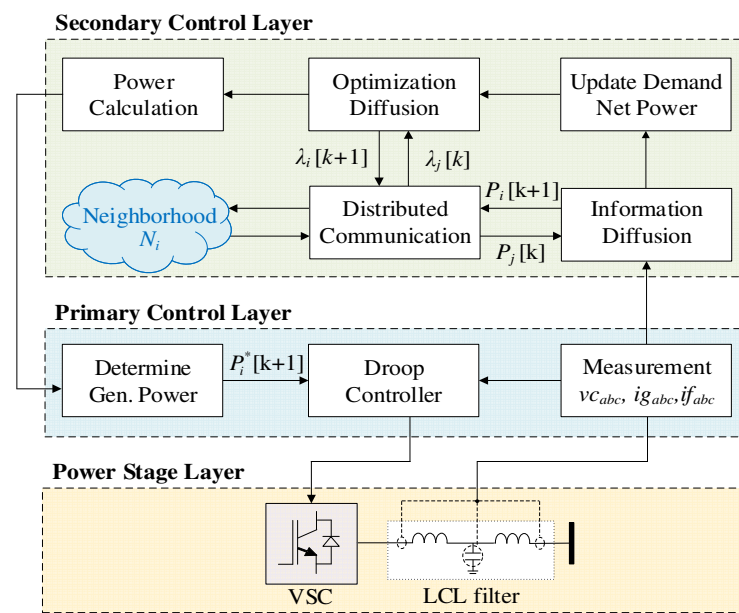


Figure 3. Block diagram of the proposed control structure.

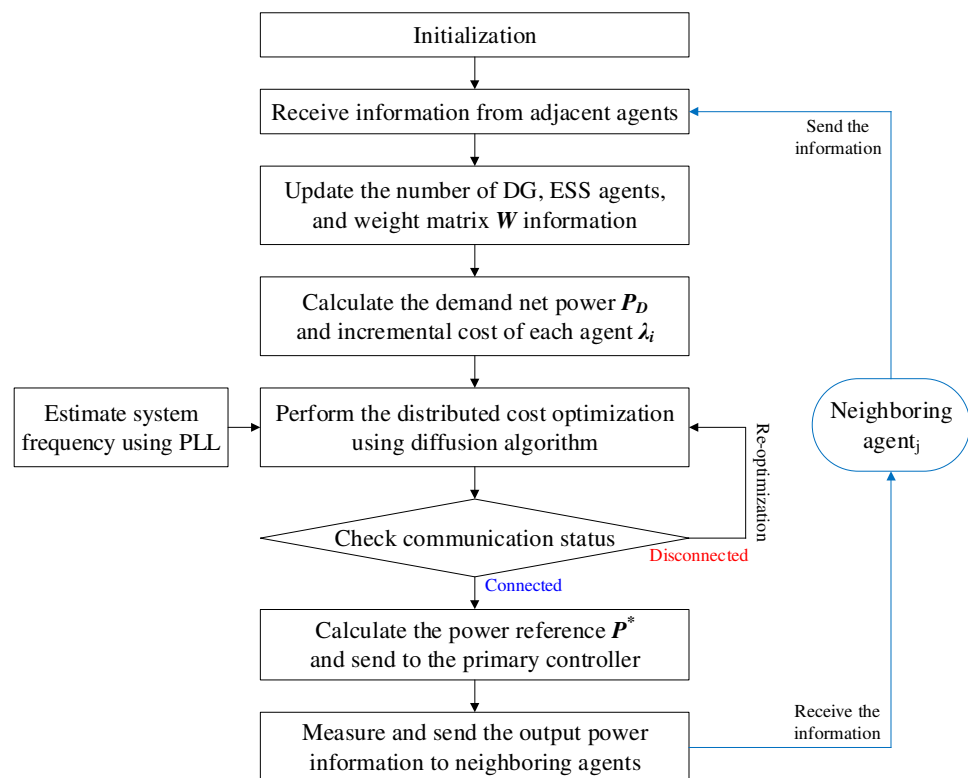


Figure 4. Flow chart of the proposed control strategy.

3.1. Primary Control

The primary controller is responsible for the power demand balance and maintenance of power quality in islanded operations. In this study, a voltage control mode (VCM) based converter was used to generate voltage by itself. The inner current and voltage control loop of the VCM converter are shown in Figure 5b. A proportional-integral (PI) regulator is

utilized to adjust the current and voltage of the converter. The current control loop is based on the decoupling of the dq -reference frame, as given by (7) and (8).

$$U_d^* = k_{pd}(i_d^* - i_d) + \int k_{id}(i_d^* - i_d)dt - \omega L_f i_q \tag{7}$$

$$U_q^* = k_{pq}(i_q^* - i_q) + \int k_{iq}(i_q^* - i_q)dt - \omega L_f i_d \tag{8}$$

where U_d^* and U_q^* are the output voltage reference; k_{pd} and k_{id} are PI coefficients of the inner controller of d axes; k_{pq} and k_{iq} are PI coefficients of the inner controller of q axes; and i_d^* and i_q^* are the current reference of the measured currents i_d and i_q of d and q axes.

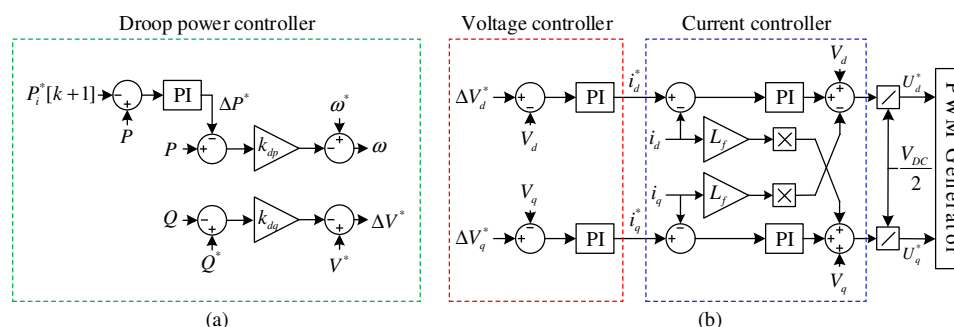


Figure 5. Control loop diagram of the primary controller: (a) Outer controller; (b) Inner controller.

The outer controller is based on a droop control scheme for power sharing among multiagent systems, as shown in Figure 5a. The droop controller calculates a reference value for angular frequency and deviation of the amplitude voltage of the inner controller, as given by (9) and (10). The system angular frequency is correlated with the active power, and the difference of the system voltage amplitude is affected by the reactive power.

$$\omega = \omega^* - k_{pg}(P - \Delta P^*) \tag{9}$$

$$\Delta V^* = V^* - k_{qg}(Q^* - Q) \tag{10}$$

where ω and ΔV^* are the angular frequency and deviation of amplitude voltage, respectively; k_{pg} and k_{qg} are the droop control coefficients; ΔP^* and Q^* are the deviation of active power and reactive power reference, respectively; and P and Q are the measurements. The deviation of power reference value for the power controller is received from the secondary control layer.

3.2. Proposed Diffusion-Based Distributed Secondary Control

The diffusion algorithm is applied for a fast convergence speed in the distributed control system. The operating cost of the MG system can be minimized if the incremental cost of all agents converges to the same value. Thus, the purpose of the diffusion algorithm is to implement an updated rule, which converges the shared information state of all agents to the same value. The agent can be considered one of the nodes in the communication network system that performs updates through the exchange of local information with adjacent nodes. Graph theory was used to describe the communication network of the diffusion-based distributed secondary controller. The communication topology can be represented as an undirected graph $G = (N, \epsilon)$ with the set of nodes $N = \{1, 2, \dots, n - 1, n\}$ and the set of edges $\epsilon \in N^2$, in which n represents the number of agents and the edges set ϵ represents the communication network established between these agents. The adjacency matrix for an undirected graph G is denoted by $A = \{a_{i,j}\}_{i,j=1,\dots,n} \in \mathbb{R}^{n \times n}$, as given by (11).

$$a_{ij} = \begin{cases} 1 & \text{if } (i, j) \in \epsilon \\ 0 & \text{if } (i, j) \notin \epsilon \text{ or } i = j \end{cases} \tag{11}$$

The Laplacian matrix $L = \{l_{ij}\}_{i,j=1,\dots,n} \in \mathbb{R}^{n \times n}$, which is a matrix form of an undirected graph G , is given by (12).

$$l_{ij} = \begin{cases} \sum_{i \neq j, j=1}^n a_{ij} & \text{for } i = j \\ -a_{ij} & \text{for } i \neq j \end{cases} \tag{12}$$

The diffusion strategy proceeds in two steps, which are information sharing and cost optimization, as shown in Algorithm 1. The first step is to calculate the total demand load of the MG system, based on the shared information between the neighboring agents. The diffusion algorithm derives the average power demand, which can calculate the total net power demand. The second step is to compute the reference power of the agent, to minimize the generation cost based on the diffusion algorithm. In this step, if a communication failure is detected, the frequency control coefficient according to the incremental cost is adjusted to maintain economic operation. Finally, the outputs of all agents are updated to the demanded net power, which is obtained in step 1.

The global dynamic combine-then-adapt (CTA) diffusion method is applied to local information sharing, to achieve an agreement on the demand load required for the MG system from dispatchable agents, as given by (13).

$$CTA_{diffusion} = \begin{cases} \phi[k] = (I - \varepsilon L)X[k] \\ X[k + 1] = \phi[k] - \mu \nabla \phi[k] \end{cases} \tag{13}$$

where $\phi[k]$ is the intermediate variable for i at time k ; $X_k = [x_{1,k}; x_{2,k}; \dots; x_{N,k}]$ is the state of agent unit i at time k ; $\mu \in \mathbb{R}^+$ denotes the non-negative update parameter of each agent; ε is constant edge weight; and $\nabla \phi[k]$ is the stochastic gradient of variable $\phi[k]$ for unit i of the intermediate value at time k .

The stochastic gradient of a diffusion strategy is simply computed as the difference between one iteration and another. Thus, the agent tracks the gradient and periodically updates the combination of its neighbor agents. The CTA diffusion was applied to the optimization of distributed operation, by adopting the gradient term of the agent incremental cost, as given by (14).

$$CTA_{Optimization} = \begin{cases} \phi[k] = (I - \varepsilon L)\lambda[k] \\ \lambda[k + 1] = \phi[k] - \mu \nabla \phi[k] - \eta \Delta f \end{cases} \tag{14}$$

where $\lambda[k] = [\lambda_1[k]; \lambda_2[k]; \dots; \lambda_{N-1}[k]; \lambda_N[k]]$ are the incremental costs of agent unit i at time k ; η_c is the frequency coefficient; Δf is the deviation of system frequency.

If the Laplacian matrix l_{ii} has a value of 0, this means that the agent is isolated from the communication network. Since the agent cannot receive information from other agents, the incremental cost cannot fully converge. Thus, the agent that detects a communication failure adjusts the frequency coefficient to reach the average incremental cost of the other agents. The frequency coefficient of an isolated agent is proportional to its incremental cost of per unit (PU), as given by (15) and (16).

$$\eta = \begin{cases} \eta_c & \text{if } l_{ii} > 0 \\ \eta_d & \text{if } l_{ii} = 0 \end{cases} \tag{15}$$

$$\eta_d = \begin{cases} \left(\lambda_i^{PU}(n-1) / \sum_{i \neq k, k=1}^n \lambda_k^{PU} \right) \cdot \eta_c & \text{if } \lambda_i^{PU} \leq \sum_{i \neq k, k=1}^n \lambda_k^{PU} \\ \left(\sum_{i \neq k, k=1}^n \lambda_k^{PU} / \lambda_i^{PU}(n-1) \right) \cdot \eta_c & \text{if } \lambda_i^{PU} > \sum_{i \neq k, k=1}^n \lambda_k^{PU} \end{cases} \tag{16}$$

where λ_i^{PU} is the incremental cost per unit of generation.

Algorithm 1: Proposed diffusion Strategy for Secondary Controller

```

1: Initialization of values
2: Updates weight matrix W
3: Step 1: Calculate shortage power ( $P_s$ )
4: While  $error_1 <$  acceptable value do
5:   for all  $i < N$  do
6:      $\phi_i[k] = \sum_{j \in N_i} \omega_{ij} P_j[k]$ 
7:      $P_i[k+1] = \phi_i[k] - \mu_i \nabla \phi_i[k]$ 
8:   end
9: end while
10: Determine dem and power:  $P_D = \sum_{i=1}^n P_i[k+1]$ 
11: Step 2: Distributed optimization
12: While  $error_2 <$  acceptable value do
13:   for all  $i < N$  do
14:      $\phi_i[k] = \sum_{j \in N_i} \omega_{ij} \lambda_j[k]$ 
15:     if  $\omega_{ii} = 0$  then
16:        $\lambda_i[k+1] = \phi_i[k] - \mu_i \nabla \phi_i[k] - \eta \Delta f$ 
17:     else if  $\omega_{ii} \neq 0$  then
18:        $\lambda_i[k+1] = \phi_i[k] - \mu_i \nabla \phi_i[k] - \eta \Delta f$ 
19:     end if
20:   end
21:   Determine power reference:  $P_i^*$ 
22:   Update based on condition:  $\sum_{i=1}^n P_i^* = P_D$ 
23:   Update error
24: end while
25: return  $P_i^*$ 
26: Wait for next sampling instant

```

As a results, the proposed secondary controller regulates the frequency, while maintaining optimal operation during the communication failure. The optimal power references of DG and ESS agents are determined by the converged incremental cost value, as given by (17) and (18).

$$P_{d,DG}^*[k+1] = \frac{\lambda[k+1] - \beta_d}{2\alpha_d} \quad (17)$$

$$P_{e,ESS}^*[k+1] = \frac{\lambda[k+1] - y_e}{2x_e} - 3P_{e,ESS}^{\max}(DOD) \quad (18)$$

where $P_{d,DG}^*[k+1]$ and $P_{e,ESS}^*[k+1]$ are the distributed output references of DG and ESS agents, respectively.

The power reference of the secondary controller based on the diffusion algorithm is sent to the droop controller of the primary control layer of each agent.

4. Simulation Results

In this study, the tested five-node MG system depicted in Figure 6 was implemented in the MATLAB/Simulink environment. The distributed MAS consists of two ESS, three DGs, and three load agents. Detailed system parameters are shown in Table 1. The converter parameters, including the sampling time of control layer, are shown in Table 2. The cost parameters for the agent type corresponding to (1) and (4) are shown in Table 3. The five agents are connected in the form of a ring communication topology, as shown in Figure 7a. In this study, two case studies are conducted to demonstrate the effectiveness of the proposed strategy during communication failure. The first case considers the isolation of DG_3 due to communication failure, as shown in Figure 7b. In this case, the communication lines between ESS_1 - DG_3 and DG_2 - DG_3 are disconnected at $t = 15$ s and $t = 25$ s, respectively. The second case considers the isolation of ESS_1 due to communication failure, as shown in Figure 7c. In this case, the communication lines between ESS_1 - ESS_2 and ESS_1 - DG_3 are disconnected at $t = 15$ s and $t = 25$ s, respectively. It is assumed that the initial loads ($Load_1$ and $Load_2$) are a total of 5kW and an additional load ($Load_3$) of 4 kW is inserted into the MG system at $t = 35$ s.

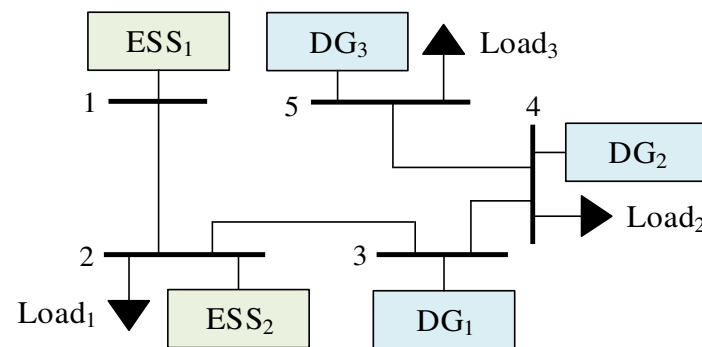


Figure 6. Tested five-node distributed MG system.

Table 1. System parameters.

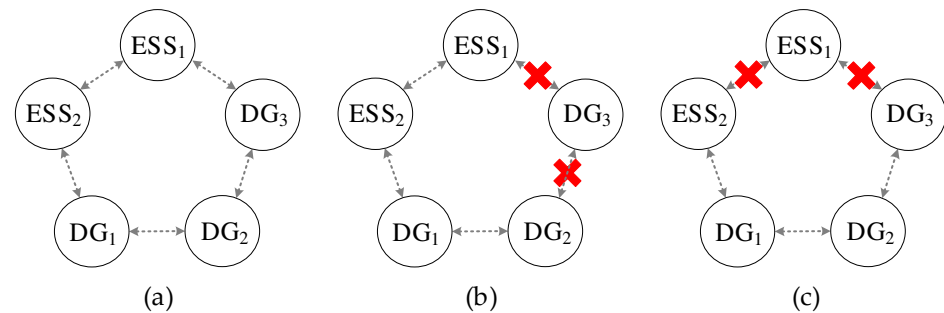
Symbol	Parameter	Value
V^*	System voltage	380 V
f^*	System frequency	60 Hz
L_f	Filter inductance	2 mH
C_f	Filter capacitance	30 μ F
R_l	Line resistance	0.0355 Ω
L_l	Line inductance	0.15 mH
L_1	Load ₁	3 kW
L_2	Load ₂	2 kW
L_3	Load ₃	4 kW

Table 2. Converter parameters.

Symbol	Parameter	Value
T_s	Sampling time	50 μ s
T_{com}	Communication time	0.05 s
k_{sp}	P gain of secondary controller	0.01
k_{si}	I gain of secondary controller	6

Table 3. Generation cost parameters.

Agent Unit	α_i (\$/kW ² h)	β_i (\$/kW ² h)	γ_i (\$/kW ² h)
ESS ₁	0.00139	3.21	382
ESS ₂	0.00144	3.37	368
DG ₁	0.00213	3.85	270
DG ₂	0.00228	3.91	246
DG ₃	0.00243	3.97	213

**Figure 7.** Communication topology: (a) Normal state; (b) DG₃ isolated; (c) ESS₁ isolated.

4.1. Case 1: DG₃ Agent Isolation According to a Communication Failure

In this case, the communication lines between ESS₁-DG₃ and DG₂-DG₃ are disconnected at 15 s and 25 s due to communication failure. The incremental cost of each agent is shown in Figure 8. As the communication line between ESS₁-DG₃ is isolated at 15 s, the communication system is converted from a ring topology to a line topology, and the re-optimization process is performed. The conventional strategy takes about 7 s for the incremental cost to converge, whereas the proposed strategy takes about 4 s. The communication line between DG₂-DG₃ fails and DG₃ is isolated at 25 s. As DG₃ is an isolated state due to the communication failure, it cannot exchange information between agents. In the conventional consensus strategy in [26], the secondary controller of the isolated agent is deactivated and the droop controller operates. Thus, the incremental cost does not converge, as shown in Figure 8a. However, the proposed diffusion strategy responds to the communication failures through a frequency regulation process based on the incremental cost information. The incremental cost of all agents converges even if DG₃ is isolated at 25 s, as shown in Figure 8b. The load inserted at 35 s results in a transient output power. The incremental costs always converge to maintain optimal operation. Figure 9 shows the outputs of all agents. The steady-state output of each agent is consistent with the Lagrange multiplier method. The proposed strategy determines the generation power reference and satisfies the demand load balance by sending it to each agent.

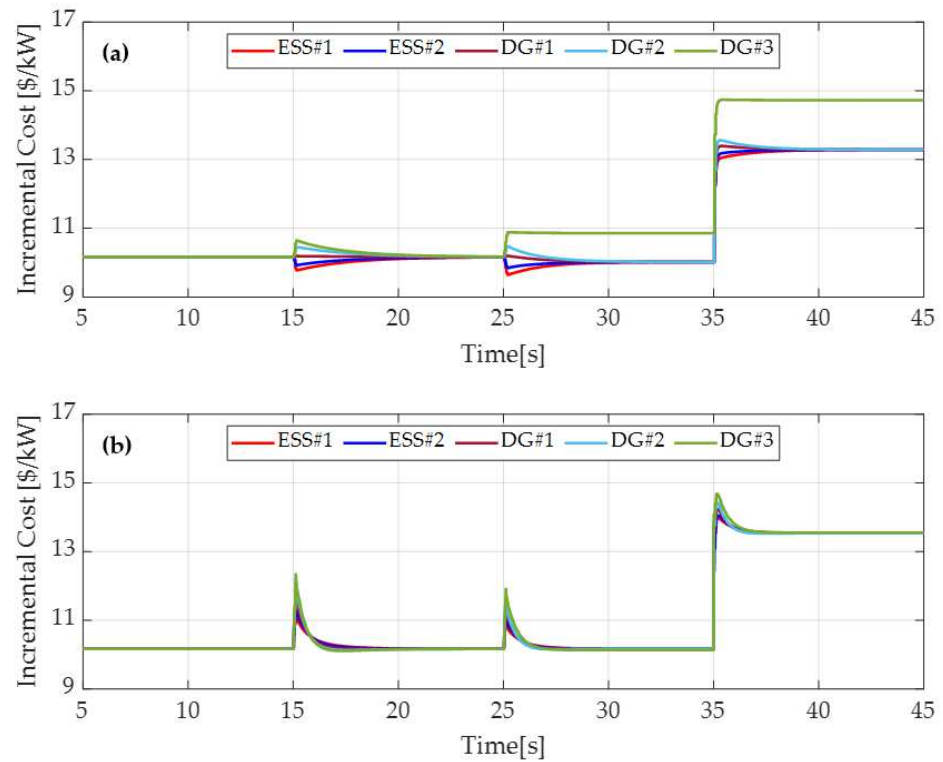


Figure 8. Incremental cost for the isolated DG_3 : (a) conventional consensus strategy; (b) proposed diffusion strategy.

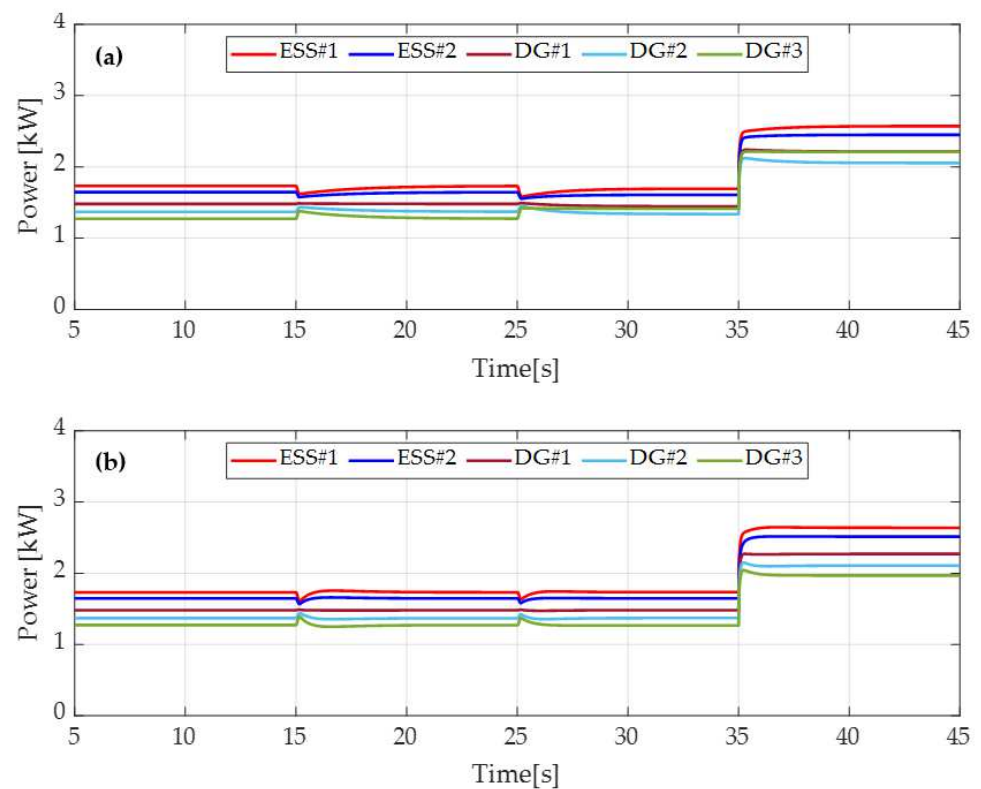


Figure 9. Output power for the isolated DG_3 : (a) conventional consensus strategy; (b) proposed diffusion strategy.

4.2. Case 2: ESS_1 Agent Isolation According to the Communication Failure

In this case, the communication lines between ESS_1 - ESS_2 and ESS_1 - DG_3 are disconnected at 15 s and 25 s, due to communication failure. The incremental cost of each agent is shown in Figure 10. As the communication line between ESS_1 - ESS_2 is isolated at 15 s, the re-optimization process is performed to maintain optimal operation. Since the weight matrix is adjusted according to the communication connection state, the incremental cost of both control schemes converges. The communication line between ESS_1 - DG_3 fails, and ESS_1 is isolated at 25 s. In the case of the conventional consensus strategy, the incremental cost convergence point of the remaining agents increases, as the ESS_1 with a low incremental cost is isolated, as shown in Figure 10a. Thus, the incremental cost of the agents does not converge, and optimal operation fails. On the other hand, the proposed diffusion strategy maintains optimal operation by deriving the incremental cost of the isolated agent through a frequency-based error adjustment process. Even if ESS_1 is disconnected from the system due to a communication line failure, the incremental costs of all agents always converge, as shown in Figure 10b. As the additional load of 4 kW is inserted at 35 s, the incremental cost variance of the conventional consensus strategy increases. The proposed diffusion strategy always converges the incremental costs between agents, even when the load increases during communication failure. It can be seen that the distributed system maintains cost optimization.

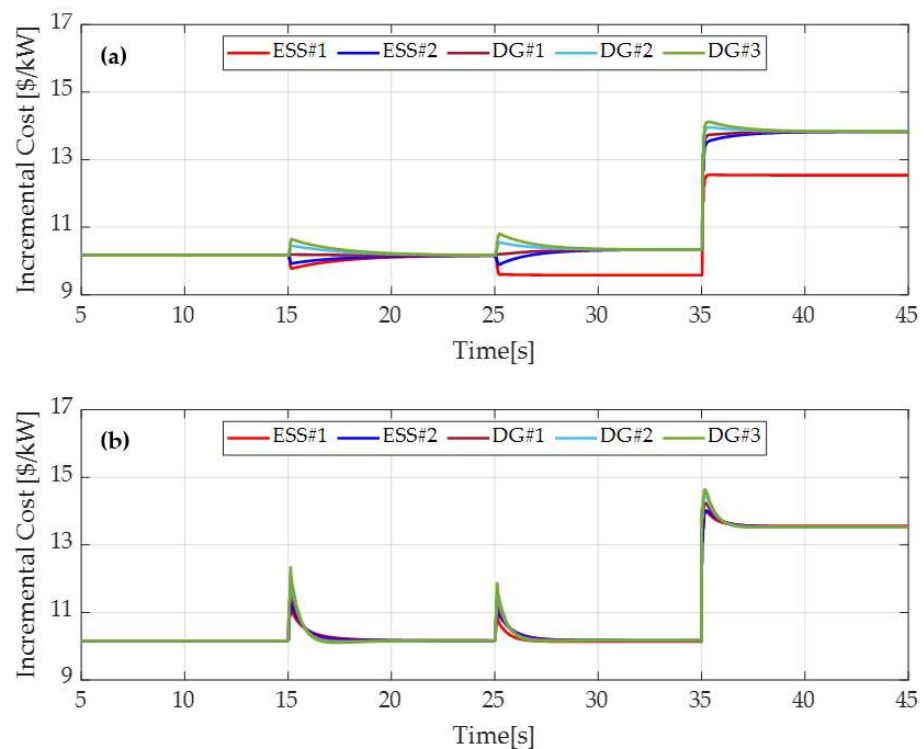


Figure 10. Incremental cost for the isolated ESS_1 : (a) conventional consensus strategy; (b) proposed diffusion strategy.

The converged incremental cost affects the response of the outputs, as shown in Figure 11. The proposed control strategy has a fast response to the generation power of the agent, due to a fast convergence speed, and can respond immediately to communication failures or load changes.

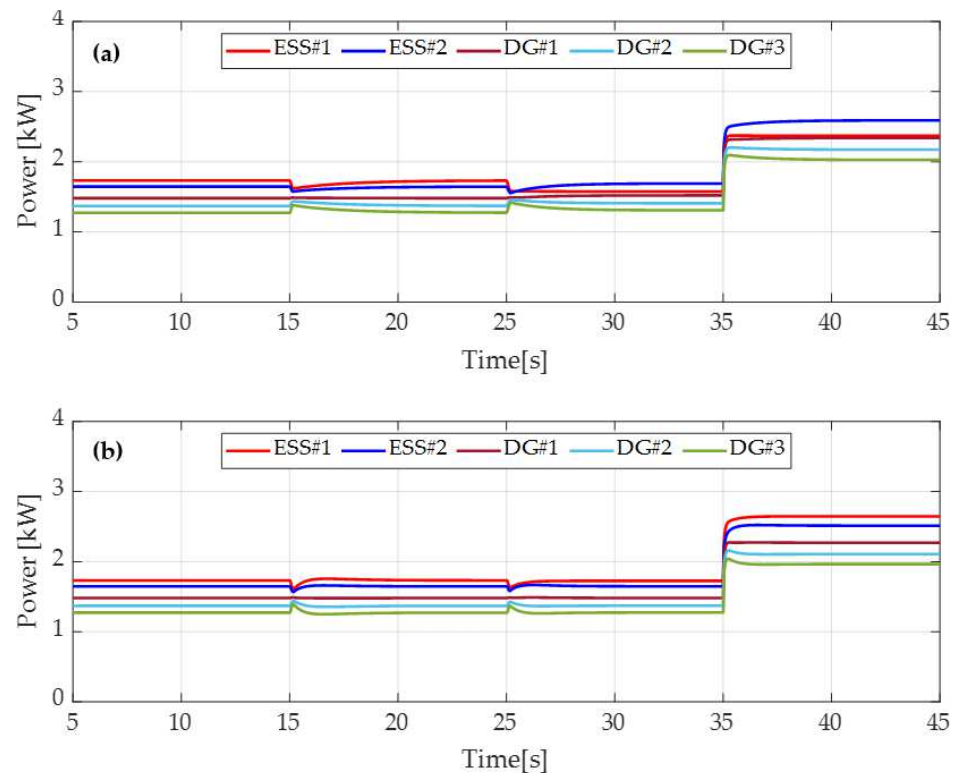


Figure 11. Output power for the isolated ESS₁: (a) conventional consensus strategy; (b) proposed diffusion strategy.

5. Experimental Results

To demonstrate the feasibility of the proposed diffusion strategy, the hardware-in-the-loop (HIL) test platform for a multiagent system was implemented using the real-time simulator OPAL-RT, as shown in Figure 12.

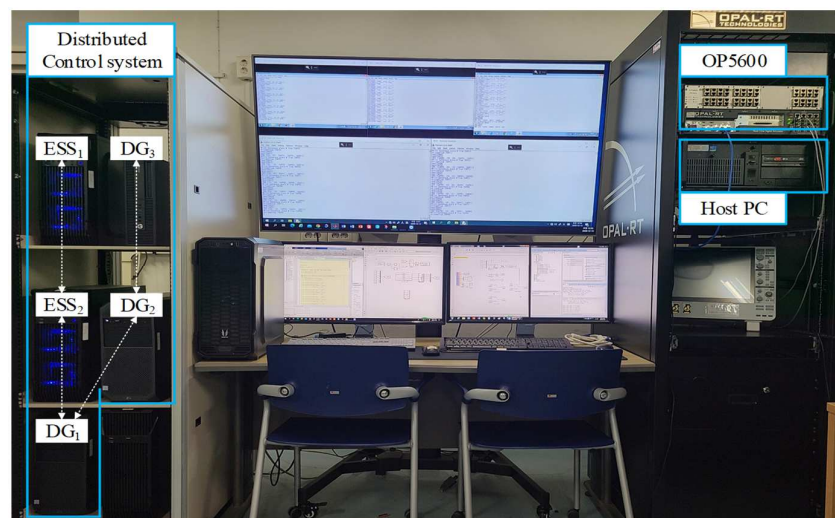


Figure 12. Real-time test platform (HIL) setup.

The tested microgrid system was implemented using RT-Lab on the host computer, then it was compiled and run in the real-time simulator OP5600. Five computers were utilized as distributed controllers of the secondary layer, and the communication topology consisted of a line connection, as shown in Figure 13. These agents used a Modbus-based Ethernet hub to communicate with the OP5600 and control PC. The diffusion-based

distributed controllers received the measured active power and battery DOD information from the real-time simulator. An optimal control operation that minimized the generation cost was performed, and the power reference was sent to the real-time simulator. The communication line disconnection between agents was implemented using a port switch in the Ethernet hub. The total test time was 240 s, and one interval was assumed to be 10 s. The unit on the x-axis was the number of hours in a day, with 24 intervals.

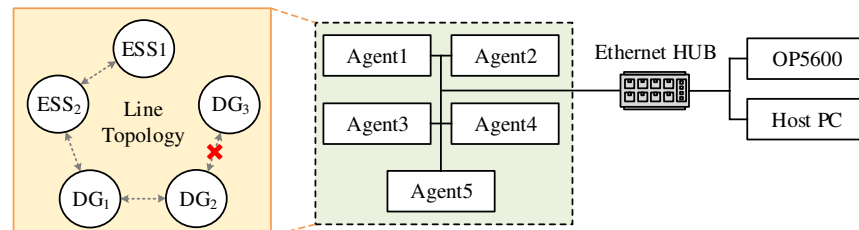


Figure 13. Communication network configuration.

A communication failure between DG_2 and DG_3 occurred for 15 intervals, from interval 6 to 21. According to the communication failure, the DG_3 was isolated from the communication network system. Figure 14 presents the incremental cost of each agent. The conventional consensus strategy has limitations in obtaining information from an isolated agent, so the incremental costs could not converge during communication failure, as shown in Figure 14a. Thus, there was a problem in optimizing distributed operation. However, the proposed diffusion strategy always converged the incremental cost, as shown in Figure 14b. Figure 15 shows the agent output power according to the converged incremental cost information. The proposed strategy sent the generation power reference to each agent.

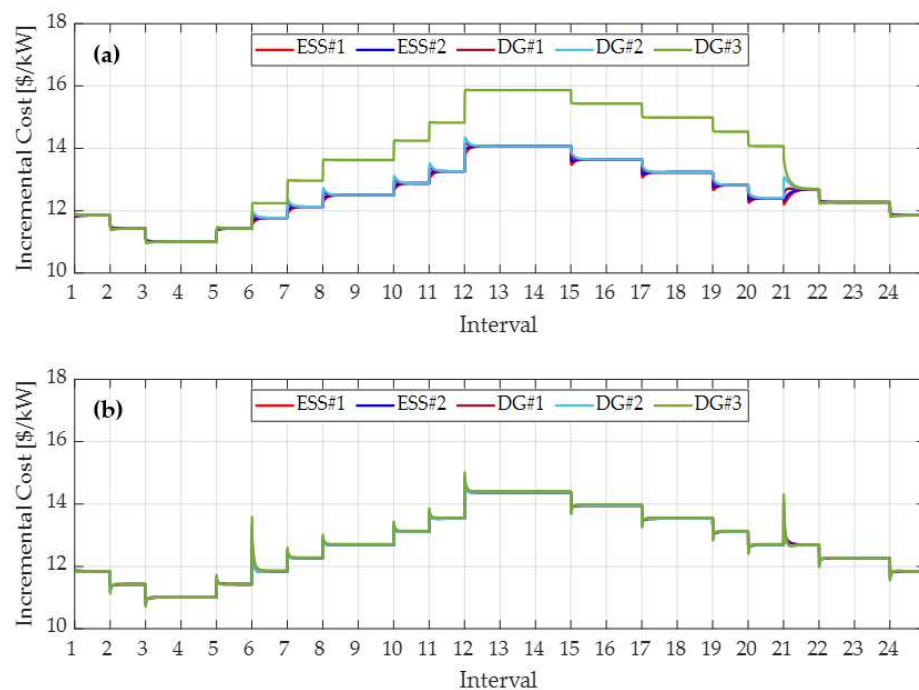


Figure 14. Incremental cost for the isolated DG_3 : (a) conventional consensus strategy; (b) proposed diffusion strategy.

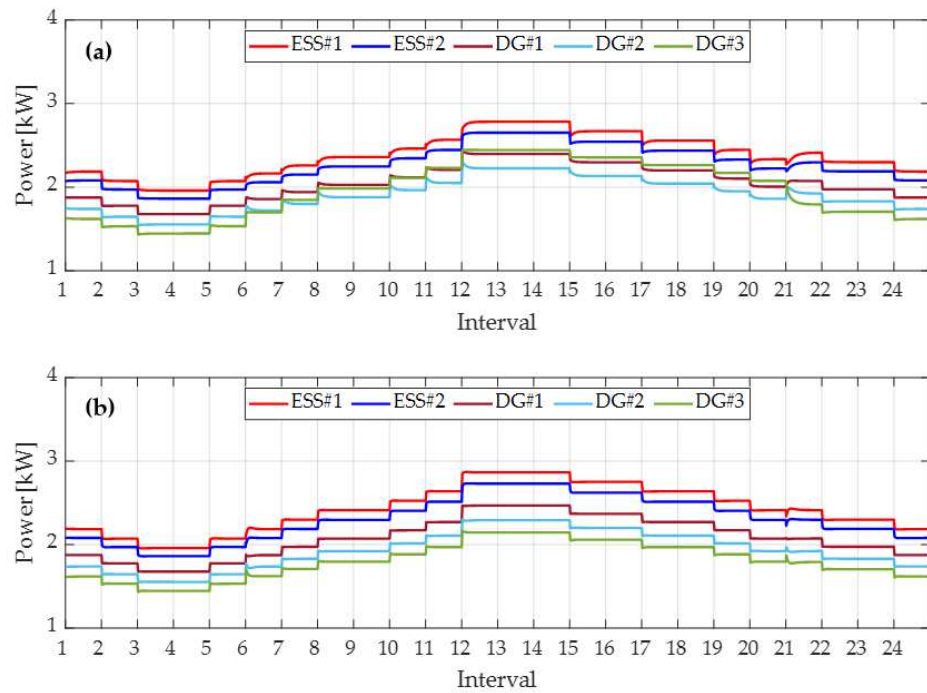


Figure 15. Output power for the isolated DG₃: (a) conventional consensus strategy; (b) proposed diffusion strategy.

The frequencies under the conventional and proposed diffusion strategy are shown in Figure 16. In the case of the conventional consensus strategy, the system frequency dropped below the nominal frequency as the load changed. This means that there was a mismatch between the system demand power and the agent supply power. However, the proposed strategy could maintain the frequency at the nominal value, without a load forecasting step in the event of load change or communication line failure.

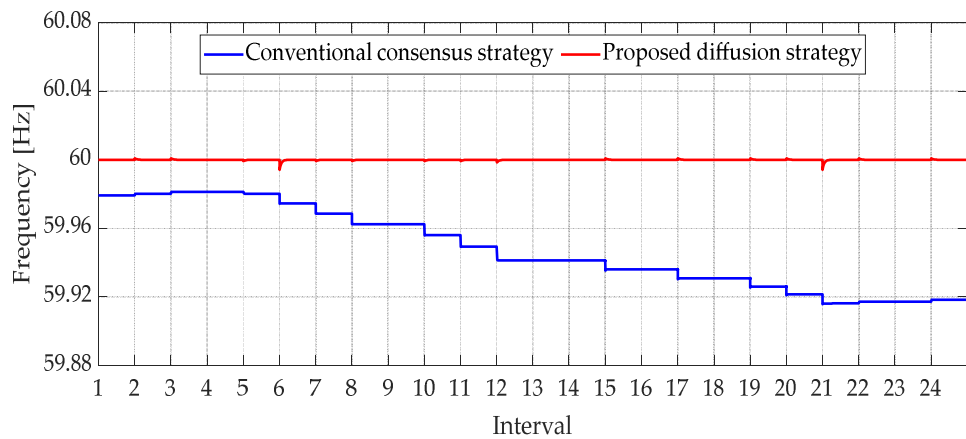


Figure 16. Comparison of system frequencies.

The comparison results of the cost optimization were compared to the conventional strategy, as shown in Figure 17. The proposed strategy maintained optimal operations during the communication failure. Table 4 shows the aggregated generation costs over 24-intervals for both control systems. The total operating costs of the conventional control strategy and the proposed control strategy were 1558.4 and 1532.5 dollars, respectively, and a cost reduction effect of about 1.69% was verified.

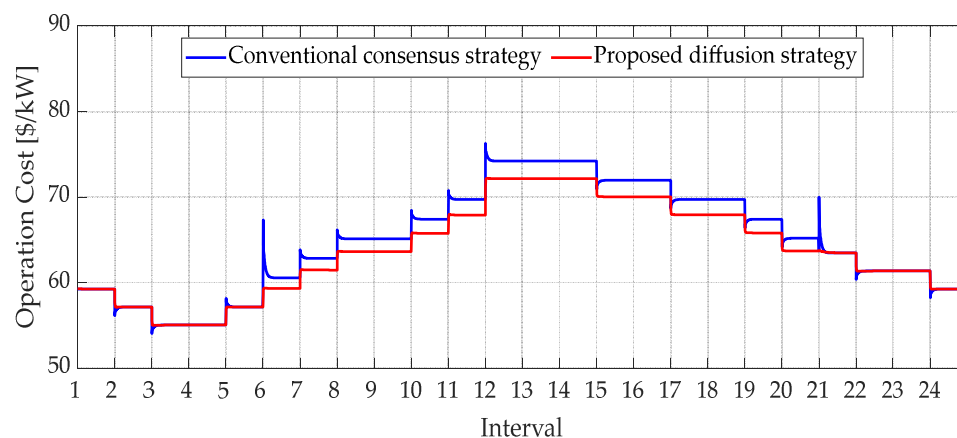


Figure 17. Comparison of total operating costs.

Table 4. Total operating cost comparison.

Control Scheme	Total Operating Cost
Conventional consensus strategy	\$1558.39
Proposed diffusion strategy	\$1532.51
Difference	1.69%

6. Conclusions

This paper proposed a distributed control strategy for a MG system. The proposed strategy performs frequency regulation and economic dispatch. The frequency coefficient is regulated based on the incremental cost rate. Thus, the proposed controller can maintain economic operation during a communication failure. The proposed strategy was simulated in two test scenarios and compared with the conventional strategy. It could minimize the generation cost, while maintaining the power balance and system frequency. A controller hardware-in-the-loop simulation was developed to validate the feasibility of the proposed diffusion strategy for practical applications. The real-time simulation results showed the superior operating performance of the proposed control strategy, in terms of cost optimization under a communication failure. Two limitations were identified in the proposed strategy. First, the number of agents separated due to communication line failure is limited. Incremental cost convergence fails, due to an error in the frequency deviation based on the number of isolated agents. Therefore, an additional compensation process for incremental cost is required, by grouping agents according to the communication connection state. The second limitation appears when communication lines are subjected to cyberattacks. Depending on the scale and type of cyber-attack, information exchanged between agents may be inaccurate or lost. In these cyber-attacks, all secondary controllers for optimal operation are disabled, and control is performed using only the primary droop controller. In the future, we will aim to overcome the two limitations of this paper.

Author Contributions: Conceptualization, investigation, and writing—original draft preparation, W.-G.L.; review, visualization and editing, T.-T.N.; review and editing and supervision, H.-M.K. All authors have read and agreed to the published version of the manuscript.

Funding: This work was supported by Incheon National University Research Grant in 2020.

Institutional Review Board Statement: Not applicable.

Informed Consent Statement: Not applicable.

Data Availability Statement: Not applicable.

Conflicts of Interest: The authors declare no conflict of interest.

References

1. Jiayi, H.; Chuanwen, J.; Rong, X. A review on distributed energy resources and MicroGrid. *Renew. Sustain. Energy Rev.* **2008**, *12*, 2472–2483. [[CrossRef](#)]
2. Akorede, M.F.; Hizam, H.; Pouresmaeil, E. Distributed energy resources and benefits to the environment. *Renew. Sustain. Energy Rev.* **2010**, *14*, 724–734. [[CrossRef](#)]
3. Mahmoodi, M.; Shamsi, P.; Fahimi, B. Economic dispatch of a hybrid microgrid with distributed energy storage. *IEEE Trans. Smart Grid* **2015**, *6*, 2607–2614. [[CrossRef](#)]
4. Che, L.; Shahidehpour, M. DC microgrids: Economic operation and enhancement of resilience by hierarchical control. *IEEE Trans. Smart Grid* **2014**, *5*, 2517–2526.
5. Hu, S.; Xiang, Y.; Liu, J.; Gu, C.; Zhang, X.; Tian, Y.; Liu, Z.; Xiong, J. Agent-based coordinated operation strategy for active distribution network with distributed energy resources. *IEEE Trans. Ind. Appl.* **2019**, *55*, 3310–3320. [[CrossRef](#)]
6. Zhang, W.; Xu, Y. Distributed optimal control for multiple microgrids in a distribution network. *IEEE Trans. Smart Grid* **2018**, *10*, 3765–3779. [[CrossRef](#)]
7. Dimeas, A.L.; Hatziargyriou, N.D. Operation of a multiagent system for microgrid control. *IEEE Trans. Power Syst.* **2005**, *20*, 1447–1455. [[CrossRef](#)]
8. Wu, T.; Xia, Y.; Wang, L.; Wei, W. Multiagent based distributed control with time-oriented SoC balancing method for DC microgrid. *Energies* **2020**, *13*, 2793. [[CrossRef](#)]
9. Lee, J.W.; Kim, M.K.; Kim, H.J. A multi-agent based optimization model for microgrid operation with hybrid method using game theory strategy. *Energies* **2021**, *14*, 603. [[CrossRef](#)]
10. Kar, S.; Hug, G. Distributed robust economic dispatch in power systems: A consensus + innovations approach. In Proceedings of the IEEE Power and Energy Society General Meeting, San Diego, CA, USA, 22–26 July 2012; pp. 1–8.
11. Wang, A.; Liu, W. Distributed incremental cost consensus-based optimization algorithms for economic dispatch in a microgrid. *IEEE Access* **2020**, *8*, 12933–12941. [[CrossRef](#)]
12. Yang, S.; Tan, S.; Xu, J.X. Consensus based approach for economic dispatch problem in a smart grid. *IEEE Trans. Power Syst.* **2013**, *28*, 4416–4426. [[CrossRef](#)]
13. Wang, R.; Li, Q.; Zhang, B.; Wang, L. Distributed consensus based algorithm for economic dispatch in a microgrid. *IEEE Trans. Smart Grid* **2018**, *10*, 3630–3640. [[CrossRef](#)]
14. Tang, Z.; Hill, D.J.; Liu, T. A novel consensus-based economic dispatch for microgrids. *IEEE Trans. Smart Grid* **2018**, *9*, 3920–3922. [[CrossRef](#)]
15. Zhang, Z.; Chow, M.Y. Convergence analysis of the incremental cost consensus algorithm under different communication network topologies in a smart grid. *IEEE Trans. Power Syst.* **2012**, *27*, 1761–1768. [[CrossRef](#)]
16. Zhang, W.; Liu, W.; Wang, X.; Liu, L.; Ferrese, F. Online optimal generation control based on constrained distributed gradient algorithm. *IEEE Trans. Power Syst.* **2014**, *30*, 35–45. [[CrossRef](#)]
17. Liu, L.; Li, B.; Guo, R. Consensus control for networked manipulators with switched parameters and topologies. *IEEE Access* **2021**, *9*, 9209–9217. [[CrossRef](#)]
18. Yang, T.; Lu, J.; Wu, D.; Wu, J.; Shi, G.; Meng, Z.; Johansson, K.H. A distributed algorithm for economic dispatch over time-varying directed networks with delays. *IEEE Trans. Ind. Electron.* **2016**, *64*, 5095–5106. [[CrossRef](#)]
19. Yuan, K.; Ying, B.; Zhao, X.; Sayed, A.H. Exact diffusion for distributed optimization and learning—Part I: Algorithm development. *IEEE Trans. Signal Process.* **2015**, *67*, 708–723. [[CrossRef](#)]
20. Yuan, K.; Ying, B.; Zhao, X.; Sayed, A.H. Exact diffusion for distributed optimization and learning—Part II: Convergence analysis. *IEEE Trans. Signal Process.* **2018**, *67*, 724–739. [[CrossRef](#)]
21. He, Y.; Wang, W.; Wu, X. Multi-agent based fully distributed economic dispatch in microgrid using exact diffusion strategy. *IEEE Access* **2019**, *8*, 7020–7031. [[CrossRef](#)]
22. Tu, S.Y.; Sayed, A.H. Diffusion strategies outperform consensus strategies for distributed estimation over adaptive networks. *IEEE Trans. Signal Process.* **2012**, *60*, 6217–6234. [[CrossRef](#)]
23. Chen, F.; Chen, M.; Li, Q.; Meng, K.; Zheng, Y.; Guerrero, J.M.; Abbott, D. Cost-based droop schemes for economic dispatch in islanded microgrids. *IEEE Trans. Smart Grid* **2016**, *8*, 63–74. [[CrossRef](#)]
24. de Azevedo, R.; Cintuglu, M.H.; Ma, T.; Mohammed, O.A. Multiagent-based optimal microgrid control using fully distributed diffusion strategy. *IEEE Trans. Smart Grid* **2017**, *8*, 1997–2008. [[CrossRef](#)]
25. Aghaee, F.; Mahdian Dehkordi, N.; Bayati, N.; Hajizadeh, A. Distributed control methods and impact of communication failure in AC microgrids: A comparative review. *Electronics* **2019**, *8*, 1265. [[CrossRef](#)]
26. Huang, B.; Li, Y.; Zhan, F.; Sun, Q.; Zhang, H. A distributed robust economic dispatch strategy for integrated energy system considering cyber-attacks. *IEEE Trans. Ind. Inform.* **2021**, *18*, 880–890. [[CrossRef](#)]
27. Rath, S.; Pal, D.; Sharma, P.S.; Panigrahi, B.K. A cyber-secure distributed control architecture for autonomous AC microgrid. *IEEE Syst. J.* **2020**, *15*, 3324–3335. [[CrossRef](#)]
28. Deng, S.; Chen, L.; Lu, X.; Zheng, T.; Mei, S.W. Event-based distributed frequency control in harsh communication conditions. *IEEE Trans. Ind. Inform.* **2022**, *18*, 3777–3786. [[CrossRef](#)]
29. Zhou, Q.; Shahidehpour, M.; Alabdulwahab, A.; Abusorrah, A. A cyber-attack resilient distributed control strategy in islanded microgrids. *IEEE Trans. Smart Grid* **2020**, *11*, 3690–3701. [[CrossRef](#)]

-
30. Fu, R.; Wu, Y.; Wang, H.; Xie, J. A distributed control strategy for frequency regulation in smart grids based on the consensus protocol. *Energies* **2015**, *8*, 7930–7944. [[CrossRef](#)]
 31. Zhao, T.; Ding, Z. Distributed finite-time optimal resource management for microgrids based on multi-agent framework. *IEEE Trans. Ind. Electr.* **2017**, *65*, 6571–6580. [[CrossRef](#)]